Optimization of reverse osmosis operational conditions to maximize ammonia removal from the effluent of an anaerobic membrane bioreactor

ARTICLE

Optimization of reverse osmosis operational conditions to maximize ammonia removal from the effluent of an anaerobic membrane bioreactor

Chungheon Shin,*[a,b,c] Aleksandra Szczuka,[a,b,d] Renjing Jiang,[a,c] William A. Mitch[a,b] and Craig S. Criddle[a,b,c]

Anaerobic membrane bioreactors can now produce effluent that meets regulatory standards for BOD, enabling energy recovery and use of the treated effluent for irrigation. RO treatment of this effluent can potentially enable recovery of potable water and total ammonia nitrogen (TAN). In this study, we optimized removal of TAN from the effluent of a Staged Anaerobic Membrane Bioreactor (SAF-MBR), a system that consists of an anaerobic fluidized bed reactor followed by anaerobic membrane bioreactor. The SAF-MBR was treated using an ESPA RO membrane. The result was a high-quality RO permeate that meets typical potable water guidelines ($\leq$ 1 mg-N/L). Hydraulic operating conditions (i.e., pressure and flux settings) did not affect TAN rejection efficiency, but pH had major impacts, due to changes in ammonium/ammonia speciation and membrane surface charge. At pH 6, TAN rejection efficiency was optimal at 99.8%. For pH > 6, passage of uncharged NH_3 increased, decreasing TAN removal. For pH < 6, the membrane retained progressively less negative (carboxylate) charge as pH decreased, decreasing ammonium removal from the optimum and allowing increased passage of ammonium into the permeate. Our results suggest that an RO membrane having a lower isoelectric point (IEP) can enable higher TAN rejection efficiencies. More concentrated RO retentate enables more efficient recovery of ammonia for reuse, and the energy required is less than the energy needed for biological removal of NH_3 as N_2 followed by synthesis of NH_3 from N_2 by the Haber-Bosch process. Further systems level research is needed to assess the energy intensity of different options for recovery and reuse of the concentrated ammonia.

Water Impacts

Anaerobic membrane bioreactors (AnMBR) coupled to reverse osmosis (RO) units enable energy and potable water recovery from wastewater. Ammonia in anaerobically treated effluent must be rejected by RO to meet reuse standards. Here, we optimize RO operation for ammonia rejection by RO membranes treating AnMBR effluent, enabling maximum ammonia recovery from RO concentrate, and low ammonia concentrations in reclaimed water.

Introduction

Energy conservation is increasingly important within the water sector.[1] In the United States, conventional domestic wastewater treatment accounts for 1 to 2 % of total U.S. electricity use.[2] This demand is largely due to energy-intensive aeration that accounts for about 50% of the energy input to conventional aerobic wastewater treatment.[1] An aeration-free alternative is anaerobic treatment using anaerobic membrane bioreactors (AnMBRs). Pilot-scale AnMBRs have achieved efficient removals of organic matter at hydraulic retention times comparable to those of aerobic processes, decreasing energy demand and providing the opportunity to recover methane for energy generation.[3] Purification of municipal wastewater effluents to potable water quality levels is increasingly important given water security concerns within the context of population growth and diminishing supplies.[4] Conventional potable reuse trains treat primary effluent with aerobic biological processes followed by Full Advanced Treatment (FAT), combining reverse osmosis (RO) with an advanced oxidation process (AOP) for efficient removal of both organic and inorganic solutes.[4,5] This processed water can potentially be reused for indirect potable reuse that incorporates an environmental buffer, such as a storage in an aquifer or a surface water reservoir, or for direct potable reuse. The energy savings associated with replacement of aerobic biological treatment with AnMBR could partially offset the energy required for FAT treatment.[6,7]

However, AnMBRs treating domestic wastewater do not remove total ammonia nitrogen (TAN) due to the absence of electron acceptors that can oxidize ammonia, such as O_2 and NO_2^-. This TAN must be removed to meet drinking water quality goals. The United States EPA has established a total nitrogen limit for US drinking water

a. Department of Civil and Environmental Engineering, Stanford University, 473 Via Ortega, Stanford, California 94305, United States
b. National Science Foundation Engineering Research Center for Re-Inventing the Nation's Urban Water Infrastructure (ReNUWIt), 473 Via Ortega, Stanford, California 94305, United States
c. Codiga Resource Recovery Center (CR2C), 692 Pampas Ln, Stanford, California 94305, United States
d. Department of Civil and Environmental Engineering, University of Michigan, 2350 Hayward St, Ann Arbor, Michigan 48109, United States

of 10 mg-N/L,[14] but individual states can impose more stringent limits as needed to address concerns related to taste and downstream disinfection.[9] In particular, chlorine added to maintain a distribution system residual will react with TAN to form chloramines. Chloramines can maintain distribution system residuals, but only ~0.6 mg-N/L TAN is needed to form ~3 mg/L of chloramine residual. Because excess free TAN can reduce water quality by promoting nitrification in distribution systems,[10] drinking water utilities typically maintain TAN < 1 mg-N/L. In North Carolina, for instance, Total Kjeldahl Nitrogen (TKN) (the sum of TAN and organic nitrogen) is limited to 1 mg-N/L. Singapore has established TAN water quality standards for its finished potable reuse water (NEWater) at < 1.0 mg-N/L.[11] Canada lacks established TAN limits for drinking water, but over 6 - 8 years of monitoring, TAN concentrations in drinking water have been consistently <1 mg-N/L, suggesting a 1 mg-N/L de facto TAN limit.[12]

To date, efforts to remove TAN from secondary municipal wastewater effluent have focused on nitritation/anammox,[13] a process that requires aeration for nitritation. Annamox bacteria use NO_2^- produced from TAN to oxidize the remaining TAN to N_2. While more efficient than conventional biological nitrogen removal, partial nitritation/anammox still requires energy to degrade TAN. Ironically, most TAN in domestic wastewater ultimately derives from the Haber-Bosch process that reduces N_2 gas to ammonia for use as a fertilizer.[14] This energy-intensive process consumes about 7% of the world's natural gas supply[15] and is responsible for 1.5% of greenhouse gas emissions worldwide.[16] Rather than consuming energy to degrade TAN back to N_2, a more sustainable alternative could be TAN recovery from anaerobically-treated domestic wastewater. However, the TAN remaining in effluents from AnMBRs (~70 mg-N/L) treating domestic wastewaters is rather dilute.[17] Concentrating TAN would facilitate TAN recovery.[18]

We recently demonstrated that RO treatment within FAT-based potable reuse trains can produce potable water while concentrating nitrate from nitrified secondary effluents in the RO retentate stream for efficient removal.[19] Using AnMBR-coupled RO within a FAT-based potable reuse train to concentrate TAN in the RO retentate stream would further improve the overall energy efficiency of the treatment train by avoiding the aeration needed for removal of organic and nitrogenous oxygen demand, and would facilitate TAN recovery, offsetting the demand for TAN production by the Haber-Bosch process.[20,21]

In order to achieve these benefits, RO operating conditions and membrane selection criteria must be optimized. Although several studies have reported TAN rejection efficiencies for RO treating aerobic secondary effluents, these studies have not addressed the underlying mechanisms of TAN rejection, and rejection efficiencies have varied widely, from 66 to 98%.[13,22,23] Only one study has reported changes in TAN rejection efficiency due to pH effects but the mechanism of TAN rejection was not addressed.[24] That study was conducted with FT30 RO (FilmTech) membranes that had a TAN rejection efficiency of 98% at pH 7.2, a removal efficiency that would meet a 1 mg-N/L standard in some cases. This efficiency is not high enough to meet TAN guidelines for AnMBRs treating domestic wastewaters with > 50 mg-N/L TAN.[21] Further improvements in removal efficiency will thus require optimization of RO operational changes and guidance on the choice of RO membrane. The TAN

rejection through an RO membrane, however, would be quite complicated because of the simultaneous effects of pH on the ammonia/ammonium speciation and the surface change of the RO membrane.[25-28] We know of no research that has examined the effects of pH on RO removal of TAN from biologically treated wastewater effluents. There is thus a need for more comprehensive testing of RO operational conditions and membrane effects on TAN removal.

The purpose of this study was to optimize RO operating conditions for treatment of AnMBR effluent, minimizing TAN in RO permeate and maximizing prospects for ammonia recovery. Using a bench-scale RO unit, we evaluated hydraulic conditions (flux and pressure) and pH effects with an ESPA RO membrane previously evaluated for treatment of secondary AnMBR effluent for potable water reuse purpose.[6] This membrane has functional groups that differ significantly from those of the FT30 membranes tested previously[24,26,27] and was recommended for water reuse applications by the manufacturer.[6]

Methods and Materials

Feed solutions

Bench-scale RO experiments carried out at different pressure and flux conditions were conducted with two solutions: an ammonium solution and anaerobic secondary effluent. The ammonium solution, prepared with NH_4Cl (Fisher Scientific) at a concentration of 47.4 mg-N/L (pH = 6.2) in deionized (DI) water, served as a baseline for comparison of TAN rejection in the absence of other constituents that could alter membrane fouling, water permeability, or TAN measurements. The anaerobic secondary effluent was obtained from a pilot-scale staged anaerobic fluidized membrane bioreactor (SAF-MBR) treating primary effluent from a microscreen (Hydro International) at the Codiga Resource Recovery Center (Stanford, CA). This is a modified version of the reactor described by Szczuka et al. and Shin et al.[6,29] The pilot-scale reactor treated ~ 20 m³/d of domestic sewage from the Stanford University campus. The SAF-MBR consisted of two anaerobic fluidized bed reactors (AFBRs) and one gas-sparged AnMBR. The hydraulic retention time (HRT) and solids retention time (SRT) of the system were 5.3 hours and 21.6 days, respectively. The gas-sparged AnMBR was equipped with two ZeeWeed 500D membrane modules (SUEZ) with a 0.04 μm nominal pore size. A net flux of 12.3 L/m²/h was maintained through these membranes. The reactor was operated as a completely anaerobic system, and electron acceptors other than SO_4^{2-} and CO_2, such as O_2, NO_2^- and NO_3^-, were not present in the influent or within the system. The long SRT ensured ammonification of organic nitrogen. TAN concentrations in the SAF-MBR effluent matched total nitrogen concentrations, indicating that TAN is the only significant nitrogen species in the effluent. Effluent samples used as influent to the RO system were 15 L-grab samples taken at the same time each morning to ensure similar effluent characteristics, and used immediately for testing. The characteristics of these samples are summarized in Table 1.

Table 1. Characteristics of SAF-MBR effluent

ARTICLE

pH	7.3 – 7.7
COD (mg/L)	60.0 – 62.0
TAN (mg-N/L)	43.6 – 64.8
Alkalinity (mg/L as CaCO₃)	237 – 316

Pilot-scale SAF-MBR effluent samples were filtered through 0.7 µm glass fiber filter papers (GF/F, Whatman) prior to RO testing to ensure removal of suspended solids that may have accumulated in the permeate line. To decrease sample pH, 95% sulfuric acid (Fisher Scientific) was added. The sulfuric acid was directly dosed to the RO feed tank.

Bench-scale RO description and operation

The bench-scale RO unit (Fig. 1) consisted of a feed tank, a pump, a chiller and three crossflow RO membrane modules. A pH probe (Fisher Accumet) and a magnetic stir bar were placed into the feed tank, and the tank was continuously mixed. A chiller was connected to the feed tank to maintain the feed water at 20°C. The pump (Hydracell, Wanner Engineering, Minneapolis, MN, USA) was equipped with a variable frequency drive (VFD). Pressure and flow rate were controlled with the VFD and manual valves mounted in the recirculation lines. Three stainless steel RO housings were used for triplicate sampling. Each RO housing had one 92 mm × 145 mm ESPA RO membrane coupon (Hydranautics, Oceanside, CA), and new membrane coupons were used for each test. RO membrane coupons were preconditioned, as described in Szczuka et al.[6] Pressure readings on each RO membrane were monitored with individual pressure gauges on retentate recirculation lines. The retentate was recirculated to the feed tank at a constant recirculation rate of 1.6 L/min, monitored with rotameters in the retentate recirculation lines. Permeate was collected at different pressure conditions to measure TAN concentrations and monitor flux. For pH tests, permeate was recirculated to maintain constant feed tank conditions, and grab samples were collected from the permeate lines for TAN analysis. Samples were collected every 15 minutes after dosing of the feed tank with H_2SO_4 to ensure that pH changes did not result from CO_2 outgassing.
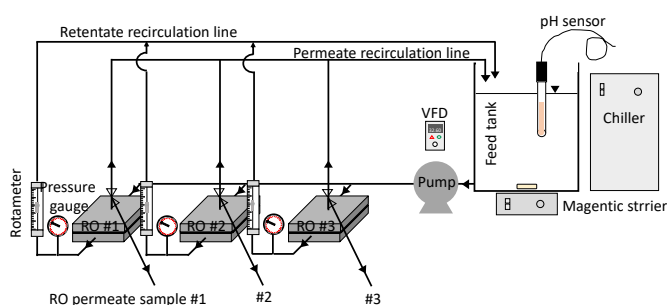

Fig. 1. Schematic diagram of the bench-scale RO unit.

Chemical analyses and calculations

All samples were triplicated from the three RO housings (Fig. 1) and analyzed immediately after sampling. HACH Method 10031 was used to measure TAN concentrations. A submerged pH probe was used to monitor the pH of feed solutions, and pH strips (Fisher Scientific) were used to monitor RO permeate pH. Alkalinity was measured by acid titration (Standard Method 2320 B) using an endpoint pH of 4.3. COD was monitored using the spectrophotometric method (EPA 410.4) with HACH Method 8000.

TAN rejection efficiency (R) was calculated with Eq. 1.

$$R \ (\%) = \frac{C^f - C^p}{C^f} \times 100 \qquad (1)$$

where C^f and C^p stand for TAN concentrations in the feed solution and RO permeate, respectively.

To calculate fractions of NH_3 and NH_4^+ in samples, the acid-base equilibrium of ammonia was considered, and the acid dissociation constant for NH_4^+, K_{a,NH_4^+}, was corrected for temperature (T, K) using Eq. 2.[30]

$$K_{a,NH_4^+} = 5.0 \times 10^{-10} \times e^{0.07 \times (T-298)} \qquad (2)$$

To calculate the solute permeability coefficient of the RO membrane, two flux conditions, water (J_w) and solute (J_s), were considered, as described by Mulder.[31] The flux of water (solvent), as indicated in Eq. 3, was calculated from permeate flow rate (Q^p) divided by membrane surface (A_m), which is equal to the water permeability coefficient (A_w) multiplied by the difference between the applied pressure (ΔP) and the osmotic pressure ($\Delta \pi$).

$$J_w = \frac{Q^p}{A_m} = A_w(\Delta P - \Delta \pi) \qquad (3)$$

The solute flux was computed using the product of permeate flow rate (Q^p) and solute concentration (C^p), divided by the membrane surface area (A_m) (Eq. 4). This is equal to the product of the solute permeability coefficient (B_s) and the difference between the solute concentrations in the feed (C^f) and permeate (C^p) solutions.

$$J_s = \frac{Q^p \times C^p}{A_m} = J_w \times C^p = B_s(C^f - C^p) \qquad (4)$$

Results

Flux and pressure effects

High molecular weight solutes and ions are typically rejected by RO membranes and thus tend to have a constant permeability coefficient, B_s, at any solution flux (J_w).[31] In this case, the solute

rejection (R) of the RO membrane is a function (Eq. 5) of A_w, B_s, and pressure conditions by solving Eqs. 1, 3 and 4.

$$R = \frac{A_w(\Delta P - \Delta \pi)}{A_w(\Delta P - \Delta \pi) + B_s} \quad (5)$$

As shown in Eq. 5, for a solute with a constant B_s, the rejection efficiency of the solute is a pressure dependent-function. Higher rejection efficiencies are achieved at higher operating pressures.[32]

For permeable non-ionic species, such as carbonic acid (H_2CO_3), boric acid ($B(OH)_3$), and ammonia (NH_3), solute rejection efficiency is not pressure dependent, and solute permeability coefficients vary depending upon flux conditions.[33] Bodalo et al. studied the permeability coefficient of TAN at a fixed pressure (39.2 bar) and flux (41.2 L/m²/h) but with variable TAN feed concentrations (55 to 9,545 mg-N/L) and reported a single permeability coefficient (4.2×10^{-4} m/h).[34] In the case of TAN, however, the permeability coefficient can vary with pressure and flux because of the presence of deprotonated non-ionic NH_3.

To evaluate the effect of pressure (or flux) on the solute permeability coefficient of TAN, the RO unit was operated at pressures ranging from 5.2 to 19.0 bar, typical pressures used for desalination of brackish water.[35] The ammonium solution used for the feed solution contained 47.3 mg-N/L TAN, a concentration similar to that of secondary AnMBR effluent, at pH 6.2. Fig. 2 illustrates water flux and TAN permeability coefficients versus applied pressure.
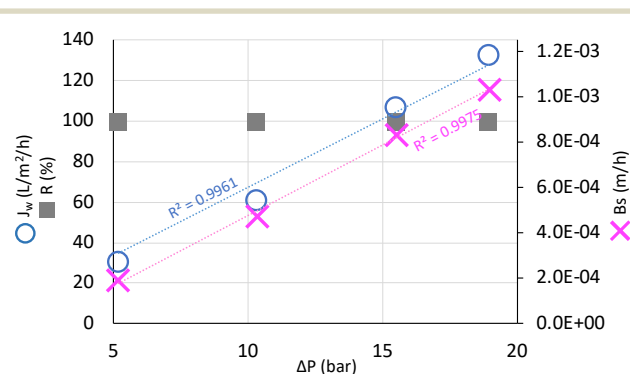

Fig. 2. Water flux (J_w), TAN rejection efficiency (R) and TAN solute permeability (B_s) at various pressure conditions (ΔP) with an ammonium solution (47.3 mg-N/L) at pH 6.2.

The water permeability coefficient (A_w) and solute rejection efficiency (R) were constant at 6.73 L/m²/h/bar and 99.2 %, respectively, while the solute permeability coefficients of TAN varied with pressure and correlated with J_w. This implies that TAN solute permeability (B_s) is governed by the solvent flux (J_w). On the other hand, TAN rejection efficiency (R) might be governed by conditions other than operational pressure or flux.

pH effects

To understand the effect of feed pH on TAN rejection efficiency by the RO unit, we varied the pH of the feed water under a constant operating pressure (10.3 bar). Effluents from the pilot-scale SAF-MBR were evaluated at pH values ranging from 3.9 to 7.9. Fig. 3 illustrates TAN rejection efficiencies at different pH values.
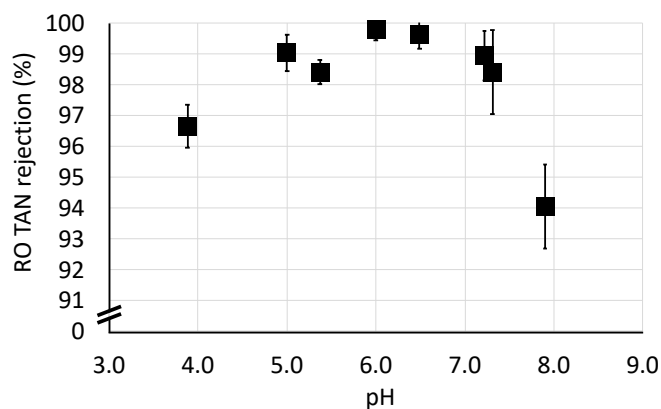
Fig. 3. TAN rejection efficiencies at different pH values. Error bars represent the standard deviation of triplicate measurements.

TAN rejections varied from 94.0 to 99.8% depending on pH. TAN rejection was highest at a pH of 6.0, at 99.8%. At pH > 6, the TAN rejection efficiency decreased because a higher fraction of uncharged NH_3 passed through the membrane. Messe et al. also reported decreased TAN rejection at elevated pH values, but also observed high TAN rejection efficiencies at pH < 6.5 (even at pH values as low as 4.61).[36] In this study, however, TAN rejection efficiencies decreased at lower pH values (pH < 6). The rejection efficiency at pH 5.4 was 98.4%, and an even lower rejection efficiency (96.6%) was observed at pH 3.9. The lower rejection efficiencies at pH > 6 is consistent with increased NH_3 due to a shift in the NH_4^+/NH_3 equilibria,[24,36] but decreased rejections at pH < 6 indicated that acid-base was not the only factor affecting TAN rejection. The data indicate that TAN rejection efficiency can be impaired in two pH zones, where different mechanisms are operative.

A zone of acid-base equilibrium of NH_4^+

In ammonia-rich solutions, a higher fraction of NH_3 is present at higher pH conditions due to a shift in the acid-base equilibrium of NH_4^+ (pK_a = 9.45 at 20°C) (Fig. 4). NH_3 and NH_4^+ speciation and TAN rejection efficiency at pH values > 6 can thus be compared.
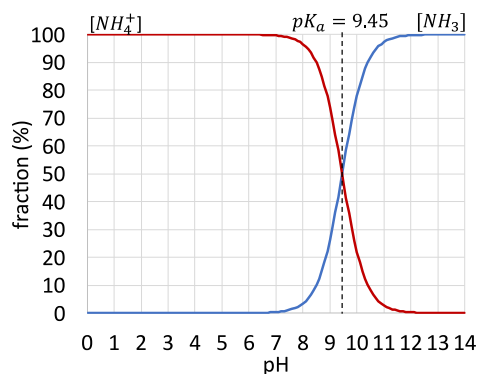
Fig. 4. NH_4^+ and NH_3 speciation at various pH conditions at 20°C.

At pH ≤ 6 and 20°C, the fraction of NH_4^+ in solution exceeds 99.96%. At pH > 6, the fraction of NH_3 is more significant, and TAN rejection efficiency decreases, as demonstrated by plotting the fraction of NH_4^+ present in solution and TAN rejection (Fig. 5).
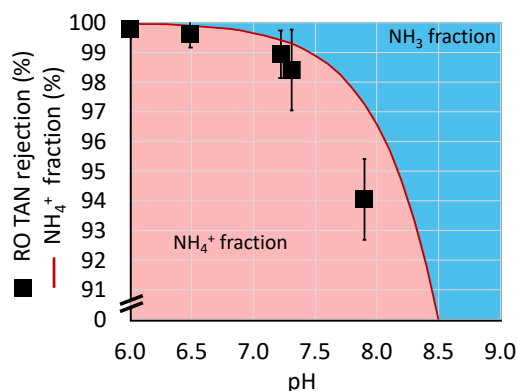

Fig. 5. Correlation between TAN rejection efficiency and NH_3 and NH_4^+ fraction at pH > 6. Error bars represent the standard deviation of triplicate measurements.

As shown in Fig. 5, TAN rejection efficiency at pH > 6 correlated with the NH_4^+ fraction in the feed. At pH values approaching 6, the NH_3 fraction decreased and higher TAN rejection was observed.

A zone of RO membrane surface charge

The active layer of polyamide RO membranes consists of carboxylic and amine functional groups. Ionization of these groups is governed by acid-base equilibria, as summarized in Fig. 6. At pH 6, functional groups on the membrane surface are deprotonated, and the surface is negatively charged due to an increase in carboxylate groups [R-COO⁻].


Fig. 6. ESPA RO membrane; correlation between negative RO surface charge (⊖) and pH in relation to functional group changes.

Negative membrane surface charge results in electrostatic repulsion and rejection of ions.[35] The negative charge repels anions, such as HCO_3^-, resulting in high anion solute rejection, and cations, such as NH_4^+, are simultaneously rejected to maintain a charge balance.[39] At pH values below 6, TAN removal deceases as pH decreases. This can be attributed to changes in membrane surface charge and the electrokinetic potential governing electrostatic rejection of ionic species.[37,38] Essentially, the membrane surface assumes a neutral or positive charge due to an increase in protonated carboxylate groups (neutral charge) and protonated amine groups (positive charge). Decreased electrostatic repulsion at lower pH enables more ionic solutes such as monovalent ions, Na^+ and Cl^-, to pass through the membrane, as reported by Hoang et al. and Qin et al.[39,33]

The [R-COO⁻] fraction in Fig. 7 was calculated with data for ESPA membranes reported by Coronell et al.,[27] who detected two types of carboxylic groups with a negligible fraction of amine groups on the active layer of the ESPA membrane. Coronell et al. reported the total concentration of the two carboxylic groups ($C_{T,CG}$) is 0.63 M. One group has a low pKa of 3.91 ($pK_{a,CG1}$), constituting 14% (w_1) of the total number of carboxylic groups, and the second group has a higher pKa of 5.86 ($pK_{a,CG2}$), constituting the remaining 86% (w_2).[27] Based on these values, the deprotonated carboxylic groups fraction [R-COO⁻] can be calculated as a function of pH ($-\log([H^+])$), as shown in Eq. 7.

$$[R-COO^-]$$
$$= \frac{C_{T,CG}w_1\left(\dfrac{K_{a,CG1}}{[H^+]+K_{a,CG1}}\right) + C_{T,CG}w_2\left(\dfrac{K_{a,CG2}}{[H^+]+K_{a,CG2}}\right)}{C_{T,CG}}$$
$$\times 100 \quad (7)$$
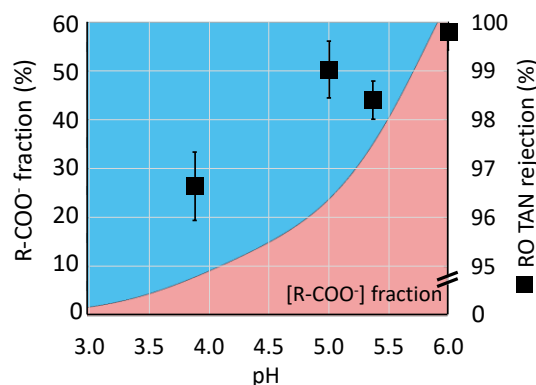
Fig. 7. Correlation between the [R-COO⁻] fraction and TAN rejection efficiency at pH < 6. Error bars represent the standard deviation of triplicate measurements.

As shown in Fig. 7, TAN rejection efficiencies decreased at lower pH. One fraction of the carboxylic acid groups deprotonates at pH values above 3.91, and the second fraction deprotonates at above 5.86. The net result is that the RO membrane surface loses negative potential at lower pH.[25,26]

Interestingly, changes in ionic NH_4^+ permeation due to changes in membrane surface charge were consistent for all pH values evaluated in this study. This was determined by comparing permeate TAN concentrations with NH_3 concentrations in the feed solution as a function of pH. Table 2 summarizes pH values, feed and permeate TAN concentrations (C^f and C^p), calculated feed NH_3 concentrations (C_{NH_3}), and the ratio of permeate TAN to NH_3 (C^p/C_{NH_3}).

Table 2. The ratio of C^p and C_{NH_3} is a function of pH.

pH	C^f (mg-N/L)	C^p (mg-N/L)	C_{NH_3} (mg-N/L)	C^p/C_{NH_3}
7.9	62.0	3.7	1.7×10^0	2
7.3	43.6	0.7	3.1×10^{-1}	2
7.2	43.6	0.5	2.6×10^{-1}	2
6.5	43.6	0.2	4.8×10^{-2}	4
6.0	62.7	0.1	2.2×10^{-2}	4
5.4	43.6	0.7	3.6×10^{-3}	192
5.0	64.8	0.8	2.3×10^{-3}	347
3.9	43.6	1.5	1.2×10^{-4}	12737

At elevated pH conditions, the C^p/C_{NH_3} ratio is smaller because a larger fraction of the TAN in the RO permeate derives from nonionic NH_3, resulting in a higher RO rejection efficiency for ionic NH_4^+. At pH > 7, the ratio of C^p to C_{NH_3} was 2, indicating that the portion of TAN in the permeate associated with NH_3 and ionic NH_4^+ was at a 1:1 ratio. This ratio doubled over the range 6.0 < pH < 6.5, where negatively charged RO membrane surface decreased. For pH values <5, these ratios were much larger at 192, 347 and 12700 at pH = 5.4, 5.0 and 3.9, respectively, implying higher fractions of TAN in the permeate from ionic NH_4^+ that had passed through the RO membrane at a less negative surface charge. This implies that pH values equal to or greater than 6 are needed to minimize passage of ionic NH_4^+ through RO membranes.

Discussion

RO membranes have different functional groups and compositions, resulting in different surface charge variations as a function of pH and different isoelectric points (IEP), the pH values where membrane surface charge is neutralized, and the negatively-charged carboxylic acid groups balance the positively-charged amine groups.[26] The effect of membrane surface charge on the rejection of both anionic and cationic solutes tends to be more intense at pH values greater than the IEP because of increased membrane surface charge, but the effect is diminished as solution pH approaches the IEP.[39]

TAN removal efficiency using the ESPA membrane can be compared with the previous study using the FT30 membrane.[24] Both membranes have different functional groups with different pK_a values, so the molar fractions of carboxylic and amine groups differ,[26,27] as summarized in Table 3.

Table 3. Summary of FT30 and ESPA RO membrane functional groups from Coronell et al. [26] and Coronell et al. [27]

RO membrane	Functional group	C_T(M)*	Subgroup	w**	pK_a	Reference
FT30	Carboxylic group	0.432 ($C_{T,CG}$)	Carboxylic group #1	0.19 (w_1)	5.23 ($pK_{a,CG1}$)	[26]
			Carboxylic group #2	0.81 (w_2)	8.97 ($pK_{a,CG2}$)	
	Amine group	0.036 ($C_{T,AG}$)	None	1	4.74 ($pK_{a,AG}$)	
ESPA	Carboxylic group	0.63 ($C_{T,CG}$)	Carboxylic group #1	0.14 (w_1)	3.91 ($pK_{a,CG1}$)	[27]
			Carboxylic group #2	0.86 (w_2)	5.86 ($pK_{a,CG1}$)	
	Amine group	N.D.***	N.D.	N.D.	N.D.	

* total concentration of carboxylic or amine group in the active layer of the RO membrane
** fraction of the functional group
*** no data because of negligible fraction of amine group compared to that of carboxylic groups

Based on the functional group information, the surface charge of the RO active layer was simulated based on the molar concentrations of the deprotonated carboxylic groups [R-COO⁻] and protonated amine groups [R-NH₃⁺] as a function of pH (Eq. 8).[28]

$$mM = -C_{T,CG} \times w_1 \left(\frac{K_{a,CG1}}{K_{a,CG1} + [H^+]} \right) - C_{T,CG}$$
$$\times w_2 \left(\frac{K_{a,CG2}}{K_{a,CG2} + [H^+]} \right)$$
$$+ C_{T,AG} \left(\frac{[H^+]}{K_{a,AG} + [H^+]} \right) \quad (8)$$

In Eq. 8, mM refers to the simulated RO membrane surface charge based on the molar concentration of the charged functional groups. The terms related to carboxylic groups are indicated with '–' to represent the negative charge from [R-COO⁻], while the terms related to the amine group are indicated with '+' to represent the positive charge from [R-NH₃⁺]. Fig. 8 compares the estimated charge variation as a function of pH with the monitored TAN rejection efficiencies for the FT30 membrane (Chen et al.)[24] and the ESPA membrane (this study).
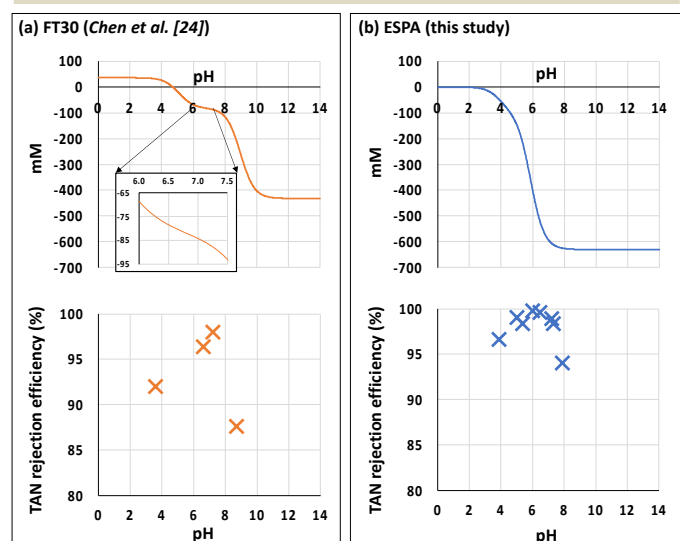
Fig. 8. Variations of the simulated RO membrane surface charge (mM) based on the charged functional groups and monitored TAN rejection efficiency, (%) as a function of bulk solution pH: (a) FT30 RO membrane (Chen et al.)[24] and (b) ESPA RO membrane (this study). The small boxed graph in (a) focuses on the mM changes over the pH range 6.0 to 7.5.

The simulated surface charges in the RO active layers (mM) of the FT30 and ESPA membranes were neutralized at pH values close to 4.7 and 2, respectively, which are close to previously reported values of 4.0 and 2.5.[40,41] Generally, the ESPA membrane had a higher molar concentration of deprotonated carboxylic acids, which resulted in a mM value for the ESPA membrane that was significantly lower than that of the FT30 membrane. For the ESPA membrane (Fig. 8(b)), maximal TAN rejection efficiency occurred at pH 6, and TAN rejection decreased as pH increased because a greater fraction of NH_3 was present in the feed solution. For the FT30 membrane [24], the maximum TAN rejection efficiency was observed at a higher pH (i.e., 98.0% at pH 7.2) than this study, but the TAN rejection efficiency decreased at pH 6.6 (96.4%). This difference in TAN rejection efficiency could be due to changes in the membrane surface charge. Although a smaller fraction of TAN is present as NH_3 at pH 6.6, the decreased negative surface charge of the FT30 membrane at pH 6.6 might allow ionic NH_4^+ to pass through the membrane. Thus, TAN rejection efficiency might be improved at a higher pH (7.2). On the other hand, operation at a higher pH yields a higher NH_3 fraction, which limits maximum TAN rejection efficiency of the FT30 membrane to 98%. Therefore, TAN rejection will be higher for RO membranes with lower IEP values that enable the membrane to retain sufficient negative charge for rejection of NH_4^+ at a pH close to 6 where uncharged NH_3 in the feed solution is negligible. RO membranes that have carboxylic acid functional groups at lower pK_a and a smaller fraction of amine groups will have a lower IEP.

Two different types of RO influents were used during this study: an ammonium solution containing NH_4Cl in deionized water, and effluents of the pilot-scale SAF-MBR treating domestic wastewater. Although the SAF-MBR effluent contained a much more complex matrix than that of the simple ammonium solution, the observed TAN removal efficiencies were similar at comparable pH: 99.8% and

99.6% at pH 6.0 and 6.5 with the SAF-MBR effluents, respectively, and 99.2 % at pH 6.2 with the ammonium solution. This indicates that a more complex feed solution has little or no adverse effect on TAN rejection efficiency, but solution pH does affect TAN rejection.

Systems level research is needed to assess the energy intensity of different options for recovery and reuse of concentrated TAN. Because TAN concentrations are low in mainstream wastewater, the potential for ammonia recovery is often viewed as unrealistically energy-intensive and costly.[18,42] This is not the case, however, when RO is used to produce potable water, and an incidental outcome is production of a concentrated TAN sidestream. Under such conditions, ammonia can cost effectively be recovered from the concentrate using conventional air stripping technology.[30] Ammonia recovery by RO/air stripping can short cut the ammonia recovery based upon conventional nitrification/denitrification to N_2 followed by Haber-Bosch synthesis of NH_3 from N_2 (Fig. 9). In current nitrogen management schemes, TAN is biologically converted to nitrate then N_2 with an energy cost of 4.2 kWh/kg-N for nitrification (assuming 12 d solids retention time; 1 kWh per kg O_2) followed by COD consumption for denitrification equivalent to loss of 9.9 kWh/kg-N (assuming 1 g COD could yield 0.0035 kWh as CH_4). The resulting N_2 is then reduced to NH_3 by the energy intensive Haber-Bosch process which requires 9.4 to 12.3 kWh/kg-N.[43] The overall result is a minimum energy cost for successive conversion of waste NH_3 to NO_3^-, NO_3^- to N_2, and N_2 to NH_3 of 4.2 + 9.9 + 9.4 = 23.5 kWh/kg-N. By contrast, ammonia in concentrated streams from RO can potentially be recovered using air stripping with reported energy requirements of 3.8 to 7.3 kWh/kg-N,[44-46] a process that would enable a maximum energy demand for NH_3 recovery of 7.3 kWh/kg-N, only one third of the energy required for conventional ammonia synthesis from waste nitrogen. Reuse or recovery of concentrated ammonia in RO retentate thus appears to be an efficient option for TAN recovery.
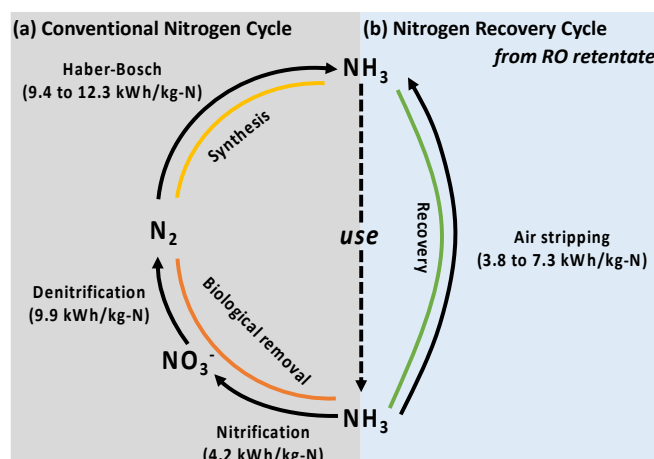
Fig. 9. (a) Conventional nitrogen cycle and **(b)** nitrogen recovery cycle from RO retentate with energy requirements (kWh/kg-N).

Conclusions

RO operating conditions were studied to elucidate optimal operating conditions that can maximize TAN rejection efficiency with effluent from a pilot-scale SAF-MBR. Hydraulic operating conditions, such as pressure and flux, did not affect TAN rejection efficiency. The operating pH, on the other hand, was a critical parameter that affected TAN rejection efficiency by controlling ammonium/ammonia speciation and RO membrane surface charge. TAN rejection efficiency (99.8%) was highest at pH 6, where the NH_3 fraction in TAN was low and sufficient negative surface charge was retained on RO membrane surface to reject ionic solutes, including NH_4^+. Membranes with low IEPs can provide higher TAN rejection efficiencies than RO membranes with high IEPs because low IEP membranes retain negative surface charge at pH conditions close to pH 6, where the fraction of ammonia present as NH_3 is minimal.

Author Contributions

Chungheon Shin: Conceptualization, Methodology, Validation, Formal analysis, Investigation, Visualization, Writing-Original Draft. **Alexandra Szczuka**: Conceptualization, Methodology, Writing-Review & Editing. **Renjing Jiang**: Investigation. **William A. Mitch**: Supervision, Writing-Review & Editing. **Craig S. Criddle**: Supervision, Writing-Review & Editing.

Conflicts of Interest

There are no conflicts to declare.

Acknowledgements

References

1   P.L. McCarty, J. Bae and J. Kim, Domestic wastewater treatment as a net energy producer–can this be achieved?, *Environ. Sci. Technol.*, 2011, **45** (17), 7100–7106.
2   C. Arzbaecher, K. Parmenter, R. Ehrhard and J. Murphy, Electricity Use and Management in the Municipal Water Supply and Wastewater Industries. Palo Alto, CA: Electric Power Research Institute and Water Research Foundation, 2013.
3   C. Shin and J. Bae, Current status of the pilot-scale anaerobic membrane bioreactor treatments of domestic wastewaters: A critical review, *Bioresour. Technol.*, 2018, **247**, 1038-1046.
4   D. Gerrity, B. Pecson, R.S. Trussell and R.R. Trussell, Potable reuse treatment trains throughout the world, *J. of Water Supply: Res. and Technol.-AQUA*, 2013, **62**(6), 321-338.
5   E.L. Marron, W.A Mitch, U.V. Gunten and D.L. Sedlak, A tale of two treatments: The multiple barrier approach to removing chemical contaminants during potable water reuse, *Acc. Chem. Res.*, 2019, **52**(3), 615-622.

6   A. Szczuka, J.P Berglund-Brown, H.K. Chen, A.N. Quay and W.A. Mitch, Evaluation of a pilot anaerobic secondary effluent for potable reuse: impact of different disinfection schemes on organic fouling of RO membranes and DBP formation, *Environ. Sci. Technol.*, 2019, **53**(6), 3166-3176.
7   H. Liu, J. Gu, S. Wang, M. Zhang and Y. Liu, Performance, membrane fouling control and cost analysis of an integrated anaerobic fixed-film MBR and reverse osmosis process for municipal wastewater reclamation to NEWater-like product water, *J. Membr. Sci.*, 2020, **593**, 117442.
8   Potable Reuse Compendium, US Environmental Protection Agency (USEPA), 2017.
9   Atrazine in drinking-water: background document for development of WHO guidelines for drinking-water quality (No. WHO/SDE/WSH/03.04/32). World Health Organization, 2003.
10 T. Zeng and W.A. Mitch, Impact of nitrification on N-nitrosamine and halogenated disinfection byproduct formation within drinking water storage facilities, *Environ. Sci. Technol.*, 2016, **50**, 2964-2973.
11 NEWater Quality, https://www.pub.gov.sg/Documents/PUB_NEWater_Quality.pdf, Singapore Public Utilities Board (PUB), 2017.
12 Guidelines for Canadian Drinking Water Quality: Guideline Technical Document — Ammonia (Catalogue No H144-13/5-2013E-PDF). Water and Air Quality Bureau, Healthy Environments and Consumer Safety Branch, Health Canada, Ottawa, Ontario, 2013.
13 X. Li, S. Klaus, C. Bott and Z. He, Status, Challenges, and Perspectives of Mainstream Nitritation–Anammox for Wastewater Treatment, *Water Environ. Res.*, 2018, **90**(7), 634-649.
14 B.L. Bodirsky, A. Popp, H. Lotze-Campen, J.P Dietrich, S. Rolinski, I. Weindl, C. Schmitz, C. Müller, M. Bonsch, F. Humpenöder, A. Biewald and M. Stevanovic, Reactive nitrogen requirements to feed the world in 2050 and potential to mitigate nitrogen pollution, *Nat. Commun.*, 2014, **5**(1), 1-7.
15 B.E. Rittmann and P.L. McCarty, Environmental biotechnology: principles and applications. Tata McGraw-Hill Education, 2020.
16 L. Wang, M. Xia, H. Wang, K. Huang, C. Qian, C.T. Maravelias and G.A. Ozin, Greening ammonia toward the solar ammonia refinery, *Joule*, 2018, **2**(6), 1055-1074.
17 G. Tchobanoglous, F.L. Burton and H.D. Stensel, Wastewater engineering: treatment and reuse, Metcalf & Eddy Inc. McGraw-Hill, Inc, New York, USA. for Environmental Research Information. Cincinnati, Ohio, 2003.
18 C. Zhang, J. Ma, J. Song, C. He and T.D. Waite, Continuous ammonia recovery from wastewaters using an integrated capacitive flow electrode membrane stripping system, *Environ. Sci. Technol.*, 2018, **52**(24), 14275-14285.
19 Z. Zhang, J.F. King, A. Szczuka, Y.-H. Chuang and W.A. Mitch, Pilot-scale ozone/biological activated carbon treatment of reverse osmosis concentrate: potential for synergism between nitrate and contaminant removal and potable reuse, *Environ. Sci.: Water Res. Technol.*, 2020, **6**(5), 1421-1431.
20 G. Bowden, H.D. Stensel and R. Tsuchihashi, Technologies for Sidestream nitrogen removal. Water Environment Research Foundation, 2015.
21 C. Zhang, J. Ma, J. Song, C. He and T.D. Waite, Continuous ammonia recovery from wastewaters using an integrated capacitive flow electrode membrane stripping system, *Environ. Sci. Technol.*, 2018, **52**(24), 14275-14285.
22 E. Dialynas and E. Diamadopoulos, Integration of a membrane bioreactor coupled with reverse osmosis for advanced treatment of municipal wastewater, *Desalination*, 2009, **238**(1-3), 302-311.

23 Y. Yun, X. Zhang and Y. Wang, Study on treating of NH$_3$–N wastewater by membrane technology in a pilot plant, *Desalination Water Treat.*, 2011, **34**(1-3), 374-381.

24 Y. Chen, M.L. Chu and M.C. Shieh, pH effect on the separation of uranium fluoride effluents by the reverse osmosis process, *Sep. Sci. Technol.*, 1992, **27**(5), 557-571.

25 M. Elimelech, W.H. Chen and J.J Waypa, Measuring the zeta (electrokinetic) potential of reverse osmosis membranes by a streaming potential analyzer, *Desalination*, 1994, **95**(3), 269-286.

26 O. Coronell, B.J. Mariñas, X. Zhang and D.G. Cahill, Quantification of functional groups and modeling of their ionization behavior in the active layer of FT30 reverse osmosis membrane, *Environ. Sci. Technol.*, 2008, **42**(14), 5260-5266.

27 O. Coronell, B.J. Marinas and D.G Cahill, Depth heterogeneity of fully aromatic polyamide active layers in reverse osmosis and nanofiltration membranes, *Environ. Sci. Technol.*, 2011, **45**(10), 4513-4520.

28 Y.S. Oren and P.M. Biesheuvel, Theory of ion and water transport in reverse-osmosis membranes, *Phys. Rev. Appl.*, 2018, **9**(2), 024034.

29 C. Shin, P.L. McCarty, J. Kim and J. Bae, Pilot-scale temperate-climate treatment of domestic wastewater with a staged anaerobic fluidized membrane bioreactor (SAF-MBR), *Bioresour. Technol.*, 2014, **159**, 95-103.

30 H. Siegrist, H., M. Laureni, K.M. Udert, T. Larsen, K. Udert and J. Lienert, Transfer into the gas phase: ammonia stripping. Source Separation and Decentralization for Wastewater Management, IWA Publishing, 2013.

31 M. Mulder, Basic Principles of Membrane Technology, Kluwer Academic, Netherlands, 2003.

32 J. Heo, L.K. Boateng, J.R Flora, H. Lee, N. Her, Y.G. Park and Y. Yoon, Comparison of flux behavior and synthetic organic compound removal by forward osmosis and reverse osmosis membranes, *J. Membr. Sci.*, 2013, **443**, 69-82.

33 J.J. Qin, M.H. Oo and B. Coniglio, Relationship between feed pH and permeate pH in reverse osmosis with town water as feed, *Desalination*, 2005, **177**(1-3), 267-272.

34 A. Bodalo, J.L. Gomez, E. Gomez, G. Leon and M. Tejera, Ammonium removal from aqueous solutions by reverse osmosis using cellulose acetate membranes, *Desalination*, 2005, **184**(1-3), 149-155.

35 M.A. Alghoul, P. Poovanaesvaran, K. Sopian and M.Y. Sulaiman, Review of brackish water reverse osmosis (BWRO) system designs, *Renew. Sust. Energ. Rev.*, 2009, **13**(9), 2661-2667.

36 L. Masse, D.I. Massé and Y. Pellerin, The effect of pH on the separation of manure nutrients with reverse osmosis membranes, *J. Membr. Sci.*, 2008, **325**(2), 914-919.

37 A.E. Childress and M. Elimelech, Effect of solution chemistry on the surface charge of polymeric reverse osmosis and nanofiltration membranes, *J. Membr. Sci.*, 1996, **119**(2), 253-268.

38 A.E. Childress and M. Elimelech, Relating nanofiltration membrane performance to membrane charge (electrokinetic) characteristics, *Environ. Sci. Technol.*, 2000, **34**(17), 3710-3716.

39 T. Hoang, G. Stevens and S. Kentish, The effect of feed pH on the performance of a reverse osmosis membrane, *Desalination*, 2010, **261**(1-2), 99-103.

40 M.R. Sohrabi, S.S. Madaeni, M. Khosravi and A.M. Ghaedi, Chemical cleaning of reverse osmosis and nanofiltration membranes fouled by licorice aqueous solutions, *Desalination*, 2011, **267**(1), 93-100.

41 H.G. Park and Y.N. Kwon, Investigation on the factors determining permeate pH in reverse osmosis membrane processes, *Desalination*, 2018, **430**, 147-158.

42 H. Cruz, Y.Y. Law, J.S. Guest, K. Rabaey, D. Batstone, B. Laycock, W. Verstraete and I. Pikaar, Mainstream ammonium recovery to advance sustainable urban wastewater management, *Environ. Sci. Technol.*, 2019, **53**(19), 11066-11079.

43 G. Soloveichik, Electrochemical synthesis of ammonia as a potential alternative to the Haber–Bosch process, *Nat. Catal.*, 2019, **2**(5), 377-380.

44 A. Zarebska, D. Romero Nieto, K. V. Christensen, L. Fjerbæk Søtoft and B. Norddahl, Ammonium Fertilizers Production from Manure: A Critical Review, *Crit. Rev. Environ. Sci. Technol.*, 2015 **45**(14), 1469-1521.

45 E. Tampio, S. Marttinen and J. Rintala, Liquid fertilizer products from anaerobic digestion of food waste: mass, nutrient and energy balance of four digestate liquid treatment systems, *J. Clean. Prod.*, 2016, **125**, 22-32.

46 Y.Y. Ye, H.H. Ngo, W.S Guo, Y.W Liu, S.W Chang, D.D. Nguyen, H. Liang and J. Wang, A critical review on ammonium recovery from wastewater for sustainable wastewater management, *Bioresour. Technol.*, 2018, **268**, 749–758.